

# Synergisms between matrices and ZSM-5 in FCC gasoline non-hydrogenating upgrading catalysts

Yihui Ding<sup>a,b</sup>, Jifeng Liang<sup>b</sup>, Yu Fan<sup>b</sup>, Yonggang Wang<sup>c</sup>, Xiaojun Bao<sup>b,\*</sup>

<sup>a</sup> College of Mining Technology, Taiyuan University of Technology, Taiyuan 030024, PR China

<sup>b</sup> State Key Laboratory of Heavy Oil Processing, China University of Petroleum, Beijing 102249, PR China

<sup>c</sup> School of Chemical & Environmental Engineering, China University of Mining and Technology, Beijing 100083, PR China

Available online 28 March 2007

## Abstract

This article describes a novel non-hydrogenating FCC gasoline upgrading catalyst system consisting of a kaolin/ $\gamma$ -Al<sub>2</sub>O<sub>3</sub> binary-matrix and an active component zeolite HZSM-5. Different catalysts made from the different combinations of HZSM-5 with the three matrices (two kaolins and  $\gamma$ -Al<sub>2</sub>O<sub>3</sub>) or their binary mixtures were prepared and their catalytic performances were assessed in a continuously flowing fixed-bed reactor using FCC gasoline as feedstock. The results showed that compared with the single-matrix based HZSM-5 catalysts, the binary-matrix based HZSM-5 catalysts had much better catalytic performance. The characterization results of the acidity, specific area and pore structure properties of the catalysts revealed that the synergisms between the matrices and HZSM-5 in the acidity and pore distribution of the binary-matrix based catalysts accounted for their improved catalytic performance. Our results demonstrated that the non-hydrogenating catalyst system developed in the present investigation can convert olefins in FCC gasoline into aromatics that have higher research octane number (RON) and thus has potential application for FCC gasoline upgrading because of its excellent olefin reduction ability and RON preservability.

© 2007 Elsevier B.V. All rights reserved.

**Keywords:** FCC gasoline non-hydrogenating upgrading; Olefin reduction; Matrix; HZSM-5; Synergism

## 1. Introduction

In Asian countries, especially in China, fluid catalytic cracking (FCC) gasoline accounts for about 80% in commercial gasoline pools, and its high olefin content (usually 50–60 vol.%) becomes one of the most difficult problems to which most of the refineries are facing in producing clean vehicle fuels. To reduce the olefin content in FCC gasoline, various measures (such as optimization of the FCC process, use of new FCC catalysts, selective hydrogenation, etc.) have been adopted, but none of them enables satisfactory olefin control without loss in the gasoline research octane number (RON). Considering that the arene content in FCC gasoline is usually in the range of 10–20 vol.%, much lower than 35 vol.% as regulated by Category 3 Unleaded Gasoline of the World-Wide Fuel Charter, therefore, there is some leeway to preserve gasoline RON by converting olefins (especially C<sub>5</sub>–C<sub>7</sub> olefins)

in FCC gasoline into *i*-paraffins and aromatics that have higher RON. Inspired by the well established industrial aromatization processes such as M2-forming [1], Cyclar [2–4], Aro-forming [5] and Alpha [6] that employ ZSM-5 zeolites as catalysts to convert light alkanes into aromatics, we proposed a non-hydrogenating FCC gasoline upgrading process. Using the carefully designed catalyst consisting of a zeolite HZSM-5 and a suitable matrix, this process converts olefins in FCC gasoline into aromatics, and thus can significantly reduce the olefin content of FCC gasoline without loss in product RON. This non-hydrogenating FCC gasoline upgrading process is featured by the hydrogen-absent operation at ambient pressure, which is especially suitable for refineries where hydro-treatment capacity is limited or low-cost hydrogen is unavailable.

Herein, we report the HZSM-5 based catalyst system used in the above non-hydrogenating FCC gasoline upgrading process. Single-matrix and binary-matrix based HZSM-5 catalysts were prepared and characterized by N<sub>2</sub> adsorption and infrared (IR) spectroscopy of adsorbed pyridine and the synergetic effects between HZSM-5 and binary matrices were discussed.

\* Corresponding author. Tel.: +86 10 89734836; fax: +86 10 89734979.

E-mail address: [baoxj@cup.edu.cn](mailto:baoxj@cup.edu.cn) (X. Bao).

## 2. Materials and methods

### 2.1. Catalyst preparation

The composition of the catalysts on anhydrous basis is HZSM-5 zeolite ( $n_{\text{SiO}_2}/n_{\text{Al}_2\text{O}_3} = 25 - 30$ , Catalyst Factory of Nankai University, Tianjin, PR China) 40 wt%, matrix (either one of the two kaolins K1 and K2 from the same origins, or  $\gamma$ - $\text{Al}_2\text{O}_3$ , or K2/ $\gamma$ - $\text{Al}_2\text{O}_3$  mixtures with different mass fractions) 52 wt%, and alumina sol (Qilu Catalyst Plant, Shandong Province, PR China) 8 wt%. The properties of the different kaolins are listed in Table 1.

Firstly, HZSM-5 powders and a suitable matrix were pre-blended in a stainless-steel beater tub to obtain a mixture; secondly, a certain amount of alumina sol was added and the resulting mixture was stirred for 30 min in a high-speed beating mill; thirdly, the resulting slurry was first aged at room temperature for 2 h, then dried at 393 K for 4 h, and activated at 813 K for 4 h to obtain a catalyst precursor; finally, the catalyst precursor was crushed and sieved into particles of 20–40 meshes in size for use.

### 2.2. Characterizations

The specific surface areas and pore size distributions of the materials used and the resulting catalysts were obtained on an ASAP 2020M instrument (Micromeritics, America). Their acid strength and acid type distribution were determined by the infrared (IR) spectra of chemisorbed pyridine obtained on a Bio-rad FTS 3000 Fourier transformed IR (FTIR) spectrometer with self-supported wafers placed into an in situ IR cell. Prior to the saturation of pyridine vapor adsorption, a treatment was conducted to obtain a vacuum degree of  $10^{-5}$  Torr at 673 K for 3 h, and then the spectra were recorded at the temperatures of 473 K and 623 K to determine the weak Lewis (L) and Brönsted (B) acidities and the strong L and B acidities, respectively.

### 2.3. Catalytic reaction and products analysis

The catalytic performance assessment experiments were carried out in a flowing-type apparatus designed for continuous operation. The reactor with an internal diameter of 10 mm was filled with the catalyst sample (ca. 6.5 ml). There are three heating zones in the reactor, with the top one as the preheater. The temperature of each zone was independently controlled within  $\pm 1$  K by thermostats. The temperature of the catalytic bed was measured by a thermocouple placed inside the reactor and was kept constant ( $\pm 1$  K). The feedstock FCC gasoline (Table 2) was fed into a preheater and then to the reactor loaded

Table 1  
Chemical compositions of the two kaolins (wt%)

Sample	$\text{Na}_2\text{O} + \text{K}_2\text{O}$	$\text{SiO}_2$	$\text{Al}_2\text{O}_3$	$\text{Fe}_2\text{O}_3$
K1	0.6	48.0	37.0	0.7
K2	0.7	49.0	36.0	0.8

Note: from Jiangsu Province, PR China.

Table 2

Lumped compositions of the feed FCC gasoline

Group composition (vol.%)	
<i>n</i> -Paraffins	5.50
<i>i</i> -Paraffins	30.19
Olefins	43.48
Naphthenes	6.46
Arenes	14.36
RON	92.1
<i>S</i> ( $\mu\text{g g}^{-1}$ )	299

with a catalyst by a syringe metering pump. The assessment experiments were conducted at 0.1 MPa and 673 K. The volume hourly space velocity (VHSV) of FCC gasoline was  $5 \text{ h}^{-1}$ . After the reaction had been conducted for 1 h, the accumulated liquid product was sampled and analyzed on a SP 3420 gas chromatograph (Beijing Analytical Instruments Factory, PR China) installed with a flame ionization detector and a HP PONA capillary column ( $50 \text{ m} \times 0.2 \text{ mm}$ ). Two or three parallel experiments were conducted and the average of their results was taken as the final data.

## 3. Results and discussion

### 3.1. Catalytic performance

#### 3.1.1. Single-matrix based HZSM-5 catalysts

By combining the HZSM-5 zeolite with the different matrices kaolins K1, K2 and  $\gamma$ - $\text{Al}_2\text{O}_3$ , respectively, three catalysts were obtained and referred as ZK1, ZK2 and ZA, respectively. Their catalytic performances were assessed and the results are shown in Fig. 1. It can be seen that the three catalysts have significantly different activities for FCC gasoline upgrading, although the three matrices themselves have no obvious difference in their activities, as shown in Table 3. The two superior catalysts, ZK2 and ZA, can greatly decrease the olefin content and increase the arene content in the product gasoline.

The above results show that there may exist some synergistic effects between the different individual matrices and the

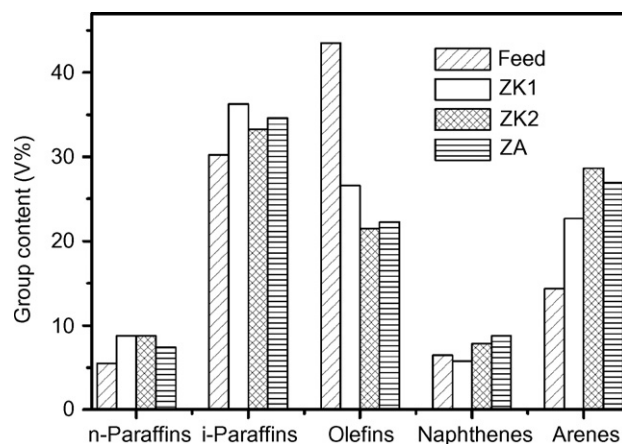


Fig. 1. Catalytic performances of single-matrix based HZSM-5 catalysts for FCC gasoline upgrading.

Table 3  
Catalytic activities of the different matrices for FCC gasoline upgrading

Catalyst	Lumped composition of the liquid products (vol.%)				
	<i>n</i> -Paraffins	<i>i</i> -Paraffins	Olefins	Naphthenes	Arenes
K1	5.42	30.62	42.05	7.07	14.85
K2	5.44	30.72	41.30	7.19	15.34
$\gamma$ -Al <sub>2</sub> O <sub>3</sub>	5.42	30.06	42.45	6.89	15.18

zeolite, which account for the differences in the catalytic performances of the catalysts made from the same active component HZSM-5 with the same content. These results suggest that fully making use of this kind of synergetic effects (e.g., by compositing the different matrices) should be of significance for enhancing the catalyst performance. It is also noted that the olefin content of the FCC gasoline after upgrading is still higher than 20 vol.% as regulated by Category 2 Unleaded Gasoline of the World-Wide Fuel Charter, so the two matrices K2 and  $\gamma$ -Al<sub>2</sub>O<sub>3</sub> used in the two superior catalysts are chosen for the further study.

### 3.1.2. Binary-matrix based HZSM-5 catalysts

To obtain a catalyst system with the desired catalytic performance, a series of binary-matrix based catalysts consisting of the same HZSM-5 with its content at 40 wt%, the binder alumina gel with its content at 8 wt%, and the binary-matrices of the different mass ratios ( $w_{K2}/w_{Al_2O_3}$ ) of kaolin K2 to  $\gamma$ -Al<sub>2</sub>O<sub>3</sub> with their contents at 52 wt% were prepared and their catalytic performances are shown in Fig. 2. It can be seen that  $w_{K2}/w_{Al_2O_3}$  strongly affects the activities of the catalysts, especially their aromatization activities. With the increasing  $w_{K2}/w_{Al_2O_3}$ , the olefin content in the products continually decreases until  $w_{K2}/w_{Al_2O_3}$  is higher than 3.0. The arene content in the products, however, shows a more complicated changing tendency with the increasing  $w_{K2}/w_{Al_2O_3}$ . For the binary-matrix based HZSM-5 catalysts, an optimum  $w_{K2}/w_{Al_2O_3}$  (equal to 1.5) exists for obtaining the maximum arene content. When  $w_{K2}/w_{Al_2O_3}$  is lower than 1.5, the arene content increases with the increasing  $w_{K2}/w_{Al_2O_3}$ ; on the contrary, when  $w_{K2}/w_{Al_2O_3}$  is higher than 1.5, the arene content decreases with the increasing  $w_{K2}/w_{Al_2O_3}$ . Furthermore, when  $w_{K2}/w_{Al_2O_3}$  is 1.5, the sulfur content in the product decreases from 299  $\mu\text{g g}^{-1}$  in the feedstock to 200  $\mu\text{g g}^{-1}$  in the product, illustrating the mild desulfurization activity of the catalyst. Except for the sulfur content, the lumped compositions of the upgraded gasoline obtained over the binary-matrix based catalyst ZKA1.5 with  $w_{K2}/w_{Al_2O_3}$  at 1.5 can measure up to the specifications of Category 2 Unleaded Gasoline of the World-Wide Fuel Charter.

The above results reveal that some synergetic interactions take place when combining the binary-matrices and the zeolite. Naturally, the question whether the synergetic effects exist between the two matrices or between the composited binary-matrices and the zeolite arises.

To answer the above question, the performance of a catalyst made from only the binary-matrix with  $w_{K2}/w_{Al_2O_3}$  at 1.5 was tested at first. The results show that the product compositions

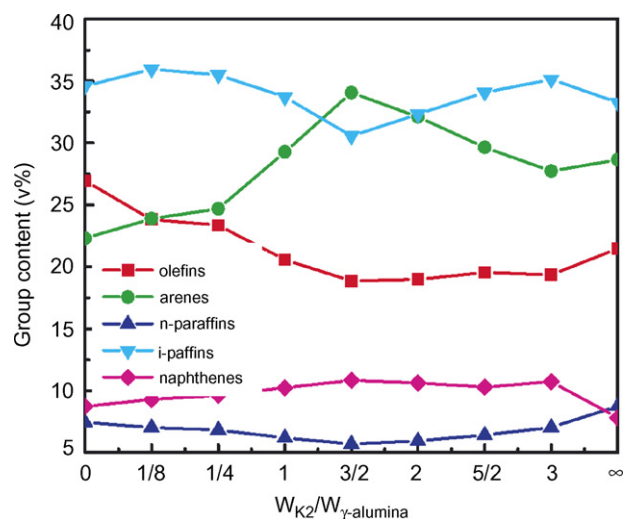


Fig. 2. Effect of  $w_{K2}/w_{Al_2O_3}$  on catalytic performances of the binary-matrix based HZSM-5 catalysts.

obtained over this catalyst were almost identical to those of the feedstock, implying that the synergetic effects between the two matrices themselves on the catalytic performance are negligible. Moreover, in view of the better aromatization activity of the binary-matrix based HZSM-5 catalyst with  $w_{K2}/w_{Al_2O_3}$  at 1.5 than those of the corresponding single-matrix based HZSM-5 catalysts (comparing Figs. 1 and 2), it can be inferred that it is the synergisms between the binary-matrix and the zeolite that contribute to the improvement in the catalytic performance of the catalysts.

### 3.2. Synergism between matrices and zeolite

To understand the synergetic effects between the zeolite and the binary matrix K2/ $\gamma$ -Al<sub>2</sub>O<sub>3</sub>, the acid properties and pore structures of the different matrices and the resulting catalysts were characterized, and their relationships with the catalytic performance are discussed as follows.

#### 3.2.1. Synergism in acidity distribution

Table 4 summarizes the acid properties of the zeolite HZSM-5, the single matrix, the K2/ $\gamma$ -Al<sub>2</sub>O<sub>3</sub> binary-matrices with different  $w_{K2}/w_{Al_2O_3}$ , and the corresponding HZSM-5 catalysts.

From Table 4, it can be seen that compared with the zeolite HZSM-5, the three matrices have much less acid amount, with the amount of L acid more than that of B acid. Among the different matrices,  $\gamma$ -Al<sub>2</sub>O<sub>3</sub> has the most total acid sites, but no B acid sites. For the two kaolin matrices K1 and K2 from the same origin, the former shows stronger acidity than the latter. As illustrated by the pathways of olefin aromatization shown in Fig. 3 [7,8], the aromatization of hydrocarbons generally involves a series of successive reactions that require not only a certain amount of the acid sites, but also the synergistic effects between B and L acid sites. Therefore, it seems difficult for either the matrices themselves or the zeolite HZSM-5 alone that have only limited amount of acid sites and/or lack the

Table 4  
Acidity distributions of the different materials and their derived HZSM-5 catalysts

Sample	Weaker acid (473 K)			Stronger acid (623 K)			Total acid			
	L <sup>a</sup>	B <sup>b</sup>	L/B	L	B	L/B	L	B	L/B	Total
HZSM-5	45.3	54.0	0.8	98.7	378.2	0.3	144.3	433.0	0.3	577.3
K1	16.8	6.1	2.8	9.0	–	–	25.8	6.1	4.2	31.9
K2	10.3	3.6	2.9	4.2	–	–	14.5	3.6	4.0	18.1
$\gamma$ -Al <sub>2</sub> O <sub>3</sub>	81.0	–	–	39.3	–	–	120.3	–	–	120.3
HZSM-5 <sup>c</sup>	13.6	16.2	0.8	29.6	113.6	0.3	43.3	129.9	0.3	173.1
KA <sub>1.5</sub>	61.9	–	–	59.9	–	–	121.4	–	–	121.4
ZK1	41.3	23.9	1.7	56.3	84.7	0.7	97.6	108.6	0.9	206.2
ZK2	42.7	29.0	1.5	53.2	50.0	1.0	95.9	79.0	1.2	174.9
ZA	44.0	19.5	2.3	101.9	76.8	1.3	145.9	96.3	1.5	242.2
ZKA <sub>0.25</sub>	71.4	27.3	2.6	89.2	38.4	2.3	160.6	65.7	2.4	226.3
ZKA <sub>1</sub>	53.3	24.2	2.2	77.5	47.5	1.6	130.8	71.7	1.8	202.5
ZKA <sub>1.5</sub>	43.2	20.5	2.1	68.5	55.9	1.2	111.7	76.4	1.5	188.1
ZKA <sub>2</sub>	47.7	22.0	2.1	60.3	60.0	1.0	108.0	82.0	1.3	190.0

Total acid ( $\mu\text{mol g}^{-1}$ ).

<sup>a</sup> L: Lewis acid ( $\mu\text{mol g}^{-1}$ ).

<sup>b</sup> B: Brönsted acid ( $\mu\text{mol g}^{-1}$ ).

<sup>c</sup> HZSM-5: HZSM-5 with its mass equal to those of the single-matrix and binary-matrices catalysts.

synergism between B and L acid sites to accomplish such a complex aromatization process. Furthermore, the linear olefins that predominate in the olefins of the FCC gasoline must undergo cyclization and hydride transfer reactions to form aromatics, nevertheless these reactions cannot be effectively catalyzed only by L acid sites [9].

The results given in Table 4 suggest that some interactions between the different matrices and the zeolite took place in the preparation processes of the single-matrix and binary-matrix based HZSM-5 catalysts. According to Choudhary et al. [10], the interactions between matrix and zeolite could change catalyst acidity distribution. In the catalyst preparation process, alkaline earth metal cations in matrix such as kaolin neutralize some zeolitic acid sites in zeolite HZSM-5, giving rise to the decrease in both the intra- and inter-crystalline acidity of HZSM-5; whereas Al species from matrix such as  $\gamma$ -Al<sub>2</sub>O<sub>3</sub> substitute the framework Si species in the zeolite to create new

zeolitic acid sites, leading to the increase in the external acidity of HZSM-5 catalyst. Accordingly, among the single-matrix based HZSM-5 catalysts, catalyst ZA with  $\gamma$ -Al<sub>2</sub>O<sub>3</sub> as matrix has the superior acidity (especially the significantly increased amount of the stronger L acid) because of the substitution of Si species in the zeolitic framework by Al species from the matrix  $\gamma$ -Al<sub>2</sub>O<sub>3</sub>, as seen in Table 4. For the two kaolin-based single-matrix HZSM-5 catalysts, catalyst ZK2 has the less amount of the total acidity (especially the less amount of the stronger B acidity) than catalyst ZK1 because of the higher concentration of alkaline oxides in the kaolin K2.

Based on the above discussion, there exist at least two effects in the binary-matrix based ZKA catalysts. One is the decrease in the stronger B acidity due to the neutralization of the zeolitic acidity by K2, and the other is the increased stronger L acidity by  $\gamma$ -Al<sub>2</sub>O<sub>3</sub>, sensing that the different proportions of K2 and  $\gamma$ -Al<sub>2</sub>O<sub>3</sub> may lead to different acidity distributions in both the acid

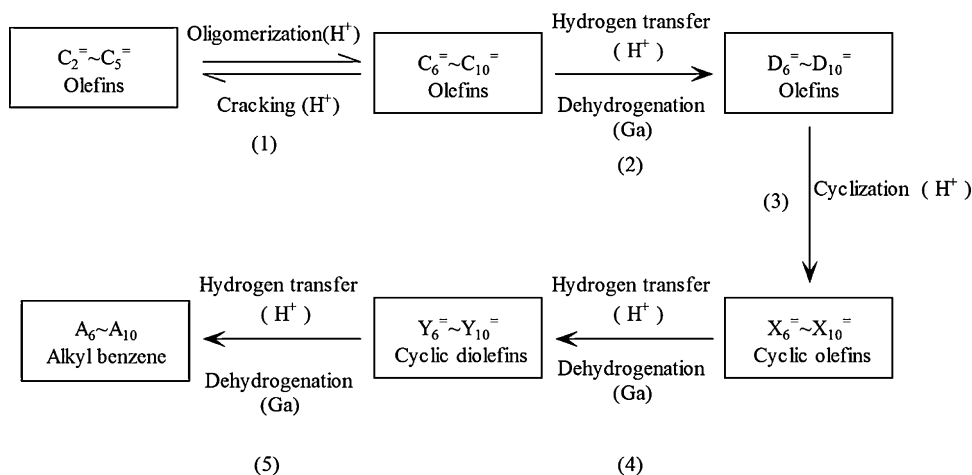


Fig. 3. Possible pathways of olefin aromatization over zeolite HZSM-5.

types and the acid amounts of the binary-matrix based ZKA catalysts. As shown in Table 4, in fact, with the increasing  $w_{K2}/w_{Al_2O_3}$ , a rather complicated acidity distribution comes to our notice that the stronger B acidity and the total B acidity increase, significantly different from the single-matrix based ones. Nevertheless, the performance of the binary-matrix based catalysts is considerably enhanced compared with that of the single-matrix based catalysts. The results confirm that among HZSM-5, K2 and  $\gamma$ - $Al_2O_3$  there exist some synergisms, although they have not been fully understood until now. However, the catalytic performance of this catalyst series is not directly related to the total acid amount, illustrating again that the acidity distribution, rather than the total acid amount, plays a more important role in FCC gasoline upgrading.

To explain the relationship between the acidity distribution and the catalytic performance of the catalysts, the ratios of L acidity to B acidity of the different catalysts are also shown in Table 4. As illustrated in Fig. 3, the aromatization of olefins, dealing with a series of reactions catalyzed by the different types of acid sites, requires the synergism between B and L acid sites. Firstly, the aromatization of olefins initiates from the formation  $C_6$ – $C_{10}$  olefins via the oligomerization of  $C_2$ – $C_5$  olefins catalyzed by B acid sites; secondly, diolefins are formed via dehydrogenation or hydrogen transfer reactions catalyzed by stronger L or B acid sites; thirdly, the cyclization of diolefins is catalyzed by B acid sites to form cycloolefins which finally yield aromatics via dehydrogenation and hydrogen transfer reactions catalyzed by L and B acid sites, respectively [11]. The composition analysis results of the feedstock show that the FCC gasoline is rich in  $C_5$ – $C_8$  olefins, so the aromatization of these  $C_5$ – $C_8$  olefins requires less B acid sites than that of  $C_2$ – $C_5$  olefins, thus making weaker the dependency of aromatization activity of the catalyst upon B acid sites. Therefore, higher ratios of L to B acidity (L/B), especially those of stronger L/B, are more favorable for olefin aromatization, just as reflected by the better catalytic performance of the two single-matrix based catalysts ZK2 and ZA that have higher ratios of both stronger L/B and total L/B (L/B > 1.0) than the single-matrix based catalyst ZK1 (L/B < 1.0).

Combining Fig. 2 and Table 4, it is observed that among the binary-matrix based catalysts, ZKA1.5 with  $w_{K2}/w_{Al_2O_3}$  at 1.5 has the most suitable ratio of L/B and thus gives the superior performance. It can be inferred that an excessive ratio of L/B means a relative insufficiency of B acid sites and thereby leads to the insufficiency of the intermediates formed from the cracking, oligomerization, and cyclization reactions catalyzed by B acid sites. Meanwhile, excessive L acid sites can accelerate the deep dehydrogenation of the aromatic precursors formed and thus evolve hydrogen to induce the hydrogenation of the olefinic and aromatic intermediates, leading to undesired declines in the yield of aromatics and the RON of the product. On the contrary, very low ratios of L/B mean too many B acid sites and too few L acid sites. In the former case, drastic cracking takes place and lower hydrocarbons formed escape in large amount; in the later case, ineffective transformation of the intermediates derived from the oligomerization and cyclization reactions into aromatics makes the dehydrogenation reactions catalyzed by L acid sites unavoidably become an aggravated bottlenecking step. Therefore, very low ratios of L/B bring about the decreases in gasoline yield and the arene content in the product.

### 3.2.2. Synergism in pore distribution

Table 5 shows that  $\gamma$ - $Al_2O_3$  has the largest specific area ( $178\text{ m}^2\text{ g}^{-1}$ ) and pore volume ( $0.48\text{ ml g}^{-1}$ ) among the three matrices. It is also seen that the macropores of 50–100 nm in diameter predominate in the two kaolin matrices and so do the mesopores of 5–20 nm in diameter in the  $\gamma$ - $Al_2O_3$  matrix. Therefore, the two kaolins and  $\gamma$ - $Al_2O_3$  can be classified into macroporous materials with small specific area and a mesoporous material with medium specific area, respectively, while the active component HZSM-5 is surely a microporous material with high specific area ( $385\text{ m}^2\text{ g}^{-1}$ ).

From Table 5, it can be seen that the specific areas and the pore volumes of the single-matrix based catalysts present a conforming relation with the parent matrices, i.e.,  $ZA > ZK1 \approx ZK2$ . It is also noted that the most probable pore diameters of the catalysts can be approximated to that of

Table 5  
Pore distributions of the different materials and their derived HZSM-5 catalysts

Sample	Specific surface area ( $\text{m}^2\text{ g}^{-1}$ )			Pore volume ( $\text{ml g}^{-1}$ )			Most probable pore diameter (nm)
	Micropore	Meso- and macro-pore	Total	Micropore	Meso- and macro-pore	Total	
HZSM-5	366	19	385	0.11	0.02	0.13	3.8
K1	–	29	29	–	0.16	0.16	70.0
K2	–	30	30	–	0.16	0.16	70.0
$\gamma$ - $Al_2O_3$	–	178	178	–	0.48	0.48	6.5
KA1.5	1	108	109	0	0.24	0.24	8.9
ZK1	76	62	138	0.036	0.075	0.111	4.0
ZK2	80	60	140	0.037	0.075	0.112	4.0
ZA	74	113	187	0.035	0.269	0.304	7.0
ZKA0.25	80	98	178	0.038	0.242	0.28	7.0
ZKA1	86	78	164	0.040	0.160	0.20	6.5
ZKA1.5	84	73	157	0.039	0.151	0.19	6.6
ZKA2	75	69	144	0.035	0.145	0.18	6.6



the parent zeolite HZSM-5, giving a decrease nearly by an order of magnitude compared with those of the pure matrices. This means that the contributions of the matrices to the specific areas and pore volumes of the catalysts above, if any, are of less importance than that of HZSM-5.

It is well known that the micropores in HZSM-5 have excellent resistance to carbon deposition [12], and the meso- and macropores in matrices can enhance the accessibility of the reactants to catalytically active acid sites and benefit the diffusion of the bulky intermediates and products. As recently reported [13], suitably compositing a mesoporous material and a zeolite could yield a hybrid catalyst that can effectively promote evacuation of the heavier aromatic products  $C_{9+}$  trapped inside the zeolite pores. Accordingly, the binary-matrix based HZSM-5 catalysts made from the macroporous K2, the mesoporous  $\gamma$ - $Al_2O_3$ , and the microporous HZSM-5 in the present investigation have a hierarchically distributed pore structure, as described by the “pore continuum” concept [13–15].

To illustrate the pore continuum and the diffusion kinetics of the binary-matrix based catalyst KA1.5, the two corresponding single-matrix based catalysts ZK2 and ZA are taken as reference for comparison. Fig. 4 shows the desorption pore volume plots of the three catalysts. One can see a narrow peak at ca. 4.0 nm for ZK2, a broad peak at ca. 7.0 nm for ZA, whereas the three peaks at ca. 4.5, 6.5 and 10.3 nm, respectively, are observed for KA1.5, evidencing the pore continuum structure of KA1.5.

Fig. 5 shows the isotherms of nitrogen adsorption and desorption obtained from the three catalysts. It reveals that the shapes of the hysteresis loops and the total volumes of adsorbed nitrogen (at relative pressure  $p/p_0 = 1.0$ ) for the three catalysts are significantly different. Within the quasi-entire relative pressure range of  $>0.0$ –1.0, the steep concave shape of the isotherms suggests that the catalysts have higher rates of adsorption or desorption, i.e., higher values of diffusivity. Fig. 5 also shows that ZA and KA1.5 have much steeper adsorption or desorption isotherms than ZK2 and thus the former two are favorable for the formation and escape of larger aromatics molecules.

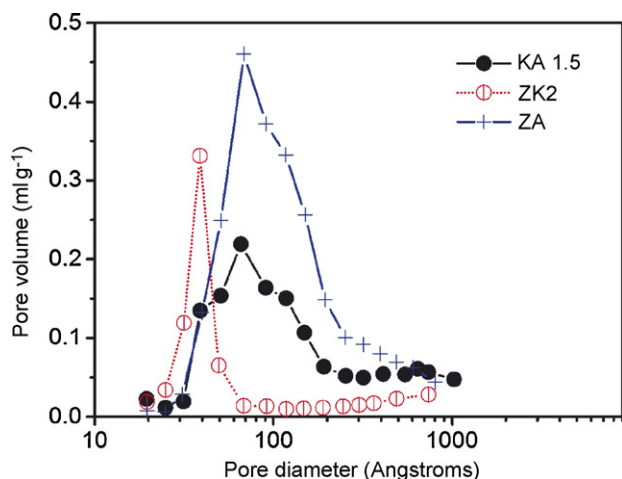


Fig. 4. Variation of the pore size distributions of catalysts ZK2, ZA and KA1.5.

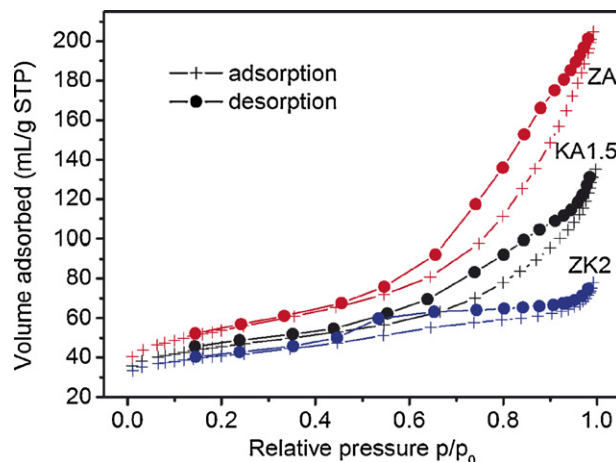


Fig. 5. Nitrogen isotherm plot of catalysts ZK2, ZA and KA1.5.

The pore structures of the binary-matrix based catalysts also accounts for their improved catalytic performance. As shown in Table 5, with the increasing  $w_{K2}/w_{Al_2O_3}$ , the specific areas and pore volumes of the catalysts decrease. When the value of  $w_{K2}/w_{Al_2O_3}$  is at 0.25, 1.0, 1.5 and 2.0, the contributions of the zeolite to the specific areas of the catalysts are 44.9%, 52.4%, 53.5%, and 52.5%, respectively, and those of the zeolite to the pore volumes of the catalysts are 13.8%, 19.7%, 20.1% and 19.9%, respectively. In the superior catalyst ZKA1.5, HZSM-5 has the largest contributions to both specific area and pore volume, signifying that both the intra- and inter-crystalline acid sites of the zeolite in the catalyst have feasibly accessible to the reactants.

#### 4. Conclusions

Considering the challenges to developing hydro-upgrading processes for FCC gasoline with high olefin content and the unavailability of low-cost hydrogen in most of the refineries in Asian countries, we proposed a non-hydrogenating FCC gasoline upgrading process and developed a kaolin/ $\gamma$ - $Al_2O_3$  binary-matrix based HZSM-5 catalyst system. This non-hydrogenating upgrading process converts olefins in FCC gasoline into aromatics that have high RON and thus provides a novel route to reduce the olefin content in FCC gasoline while preserving gasoline RON. It was found that the binary-matrices based HZSM-5 catalysts had much better catalytic performance in comparison with the single-matrix based HZSM-5 catalysts because of the synergisms between the matrices and the zeolite in both acidity and pore structure. Both the higher L/B ratio and the pore continuum are more important for achieving highly active FCC gasoline non-hydrogenation upgrading catalysts.

#### Acknowledgement

The authors acknowledge the financial support from Ministry of Science and Technology of China through the National Basic Research Program (No. 2004CB217807).

## References

- [1] N.Y. Chen, T.Y. Yan, *Ind. Eng. Chem. Proc. D.D.* 25 (1986) 151.
- [2] J.A. Johnson, J.A. Weiszmann, G.K. Hilder, A.H.P. Hall, Paper Presented at the 1984 NPRA Annual Meeting, San Antonio, TX, March 25–27, 1984.
- [3] R.F. Anderson, J.A. Johnson, J.R. Mowry, in: *Proceedings of the AIChE Meeting*, Houston, TX, March 24–28, 1985.
- [4] G. Giannetto, R. Monque, R. Galiasso, *Catal. Rev. Sci. Eng.* 36 (1994) 271.
- [5] M. Guisnet, N.S. Gnep, *Appl. Catal. A: Gen.* 89 (1992) 1.
- [6] Y. Nagamori, M. Kawase, *Micropor. Mesopor. Mater.* 21 (1998) 439.
- [7] N. Viswanadham, A.R. Pradhan, N. Ray, S.C. Vishnoi, U. Shanker, T.S.R. Prasada Rao, *Appl. Catal. A: Gen.* 137 (1996) 225.
- [8] B.L. Dmirti, N.S. Gnep, R.G. Michel, *Ind. Eng. Chem. Res.* 33 (1994) 223.
- [9] H.T. Song, W.B. Jiang, Z.J. Da, *Acta Petro. Sin.* 19 (2003) 14.
- [10] V.R. Choudary, P. Devadas, A.K. Kinage, M. Guisnet, *Appl. Catal. A: Gen.* 162 (1997) 223.
- [11] H. Guo, X. Wang, F. Yang, F. Yang, P. Zhang, Zh. Xu, R. Wang, L. Zhao, Y. Hu, *Chinese J. Mol. Catal.* 18 (2) (2004) 109.
- [12] N. Viswanadham, G. Murali Dhar, T.S.R. Prasada Rao, *J. Mol. Catal. A: Chem.* 125 (1997) 187.
- [13] R. Le Van Mao, J.H. Yao, L.A. Dufresne, R. Carli, *Catal. Today* 31 (1996) 247.
- [14] R. Le Van Mao, *Micropor. Mesopor. Mater.* 28 (1999) 9.
- [15] R. Le Van Mao, N. Al-Yassir, D.T.T. Nguyen, *Micropor. Mesopor. Mater.* 85 (2005) 176.